Atmospheric Forcing on the Barents Sea Winter Ice Extent

ASGEIR SORTEBERG

Bjerknes Centre for Climate Research, Bergen, Norway

BØRGE KVINGEDAL

Bjerknes Centre for Climate Research, and Geophysical Institute, University of Bergen, Bergen, and Statoil, Stavanger, Norway

(Manuscript received 5 May 2005, in final form 18 January 2006)

ABSTRACT

The atmospheric forcing on the Barents Sea ice extent during winter [December–February (DJF)] has been investigated for the period 1967–2002. The time series for the sea ice extent is updated and includes the winter of 2005, which marks a new record low in the wintertime Barents Sea ice extent, and a linear trend of -3.5% decade^{-1} in the ice extent was found. Covariability between the Barents Sea ice extent and the atmospheric mean seasonal flow and the synoptic cyclones has been discussed separately. For the mean flow, linear correlations and regression analysis reveal that anomalous northerly (southerly) winds prevail in the Nordic Seas during winters with extensive (sparse) Barents Sea ice extent. Some of the variability in the mean flow is captured by the North Atlantic Oscillation (NAO); however, the wintertime link between the Barents Sea ice extent and the NAO is moderate. By studying the cyclone activity in the high-latitude Northern Hemisphere using a dataset of individual cyclones, two regions that influence the wintertime Barents Sea ice extent were identified. The variability in the northward-moving cyclones traveling into the Arctic over East Siberia was found to covary strongly with the Barents Sea ice extent. The main mechanism is believed to be the change in the Arctic winds and in ice advection connected to the cyclones. In addition, cyclone activity of northward-moving cyclones over the western Nordic Seas was identified to strongly influence the Barents Sea ice extent. This relationship was particularly strong on decadal time scales and when the ice extent lagged the cyclone variability by 1–2 yr. The lag indicates that the mechanism is related to the cyclones' ability to modulate the inflow of Atlantic water into the Nordic Seas and the transport time of oceanic heat anomalies from the Nordic Seas into the Barents Sea. Multiple regression indicates that the two mechanisms may explain (or at least covary with) 46% of the wintertime Barents Sea variance over the 1967–2002 period and that 79% of the decadal part of the ice variability may be predicted 2 yr ahead using information about the decadal cyclone variability in the Nordic Seas.

1. Introduction

The amount and thickness of sea ice in the Arctic region are important factors in the global climate system. In the Barents Sea (BS), the winter [December–February (DJF)] sea ice is relatively thin compared to the rest of the Arctic Ocean. The sea ice in this area has a large annual cycle with minimum ice in September and maximum ice in April. More so, the winter sea ice extent shows interannual variability. The thin layer of ice is very sensitive to changes in both the atmosphere and the ocean. Variability in the sea ice concentration and extent may again influence the regional as well as global climate in different ways, such as through changes in albedo, momentum, heat and water vapor exchange, and deep water formation.

The Barents Sea is situated in an area with relatively high cyclone center counts (X. Zhang et al. 2004). The low pressure systems are mainly advected northward from the North Atlantic, which is an important mechanism for transporting heat and moisture from lower latitudes into the Arctic. In the context of global climate, it is generally believed that the greenhouse warming will amplify in the polar regions (Houghton et al. 2001; Hassol 2004), although this is questioned by Polyakov et al. (2002) and there are still uncertainties as to how the cyclone activities are responding to global warming. McCabe et al. (2001) and X. Zhang et al.

Corresponding author address: Asgeir Sorteberg, Bjerknes Centre for Climate Research, Allgaten 55, 5007 Bergen, Norway.
E-mail: asgeir.sorteberg@bjerknes.uib.no

(2004) seem to agree that high-latitude cyclone frequency and intensity have increased during the second half of the twentieth century. McCabe et al. (2001) showed that high-latitude cyclone frequencies correlate well (0.69) with the Arctic Oscillation (AO), which is the dominant pattern of sea level pressure (SLP) variations north of 20°N (Thompson and Wallace 1998) over the 1959–97 period.

Many studies have focused on the connection between Arctic sea ice variability and the AO or the North Atlantic Oscillation (NAO; Hurrell 1995), which essentially describes the same airmass movement. Both model studies (Zhang et al. 2000; Zhang and Hunke 2001) and observational studies (Slonosky et al. 1997; Mysak and Venegas 1998; Yi et al. 1999; Deser et al. 2000; Rigor et al. 2002; Krahmann and Visbeck 2003; Liu et al. 2004) strongly agree that at least part of the large-scale sea ice decrease in the Arctic is associated with the recent increase in the AO and NAO. However, Liu et al. (2004) pointed out that the upward AO trend during October 1978–September 2002 leads to more ice in the Kara, Chukchi, and Beaufort Seas and the Northwest Passage, which is opposite to the regional ice trends. Moreover, the magnitude of the ice changes associated with the AO is much smaller than the regional ice trends. They therefore argued that in order to fully understand the regional trends, other large-scale processes need to be considered.

Sea ice extent in the Arctic has decreased by about 3% decade^{-1} from the beginning of the satellite era (Johannessen et al. 1999; Parkinson et al. 1999). However, there are large regional differences. Using satellite data from 1978 to 1996, Parkinson et al. (1999) found that the largest regional decrease in sea ice extent, −10.5% decade^{-1}, was in the Kara and Barents Seas. Kvingedal (2005) pointed out that extrapolating such trends could lead to large errors and misinterpretations. Kvingedal (2005) found a similar trend for the same period as Parkinson et al. (1999) over the combined Greenland, Iceland, and Norwegian Seas [Nordic Seas (NOR)] and Barents and Kara Seas. However, by studying the longer 1967–2002 period in the same area, the long-term trend is less than half (−4.1% decade^{-1}) of the shorter 1978–96 trend, pinpointing how the large natural variability of the Arctic may influence short-term trends (Sorteberg et al. 2005a).

When discussing winter sea ice variability in the Arctic, the actual sites for variability are the Nordic, Labrador, Barents, and Bering Seas and the Sea of Okhotsk. Other areas in the Arctic Ocean are generally fully covered by sea ice during the winter.

The interannual variability in wintertime sea ice extent in the Nordic and Labrador Seas resembles the variability in the NAO. The conceptual picture is that the strengthening of the NAO is associated with an intensification of the Icelandic low, which leads to the advection of anomalously warm air into the Nordic Seas and subsequent sea ice melting or reduced freezing. To the west of Greenland, the advection of colder air masses will lead to increased sea ice extent in the Labrador Sea. This Labrador–Nordic Sea dipole pattern in sea ice concentration anomalies exhibits large decadal variability (Slonosky et al. 1997; Walsh and Johnson 1979; Mysak et al. 1990; Deser et al. 2000, 2002). It should be noted here that variability in the Nordic Seas is also influenced by local ice formation of the Odden feature (Vinje 1976; Comiso et al. 2001; Shuchman et al. 1998) and by the East Greenland Current's transport of thick, multiyear ice from the Arctic Ocean through the Fram Strait (Walsh and Chapman 1990; Vinje 2001b; Kwok et al. 2004).

Vinje (1998, 2001a) showed the April sea ice extent in the Barents Sea for the years 1864–1998 to be fairly well correlated with the NAO winter index. The relationship is, however, not stationary over time. For the late period 1966–96, the explained variance of the April sea ice extent is 40% while in the early period 1864–1900, only 9% could be explained by the wintertime NAO.

Clearly, some of the winter sea ice extent in the Barents Sea can be explained by the large-scale NAO. However, more local and/or less-known large-scale processes should also be investigated. An alternate dynamic mode that was shown to be a more consistent indicator of Arctic sea ice export through the Fram Strait was the phase of the atmospheric SLP planetary waves 1 and 2 (Cavalieri 2002). Also, the feedback mechanisms to the atmosphere due to the Barents Sea ice variability are of great interest. In wintertime, with large air–sea temperature differences, the (upward) turbulent heat flux from an open ocean may reach 300–500 W m^{-2}, which is almost two orders of magnitude larger than through the ice (Andreas 1980; Simonsen and Haugan 1996). Therefore, even small areas of open water (e.g., leads or polynyas) in regions normally covered by ice may well dominate the regional heat budget (Maykut 1978).

In this paper, we look at the covariability between wintertime mean circulation and the wintertime Barents Sea ice extent. In addition, the separate effect of wintertime cyclones is investigated. The wintertime Barents Sea ice extent is presented in section 3, which follows the section "Data and methods." In sections 4, 5, and 6, the relationship between the Barents Sea win-

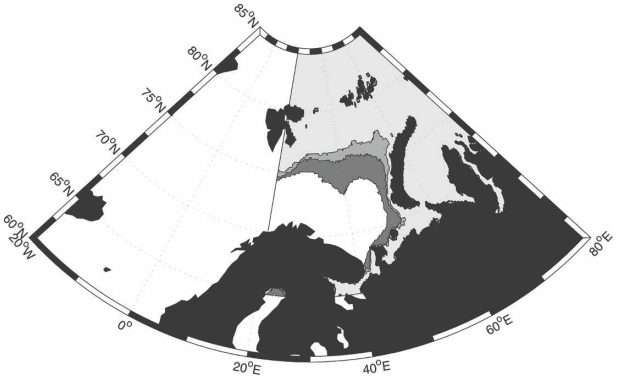

FIG. 1. Map showing the area of study and the mean winter Barents Sea ice edge (gray). Also shown are the mean ice edges for the sparse (<-1 std dev) sea ice composite (light gray) and the extended (>1 std dev) sea ice composites (dark gray).

ter ice extent and mean sea level pressure, surface air temperature, and cyclone variability is presented, respectively. The discussion and conclusions follow in section 7.

2. Data and methods

a. Sea ice data

Weekly sea ice concentration data for the Greenland and Barents Seas have been digitalized and gridded from sea ice charts, analyzed, and quality controlled by the Norwegian Meteorological Institute and the Norwegian Polar Institute. The ice charts are mapped using several different data sources such as satellite images, U.S. ice maps (Birds Eye aircraft from 1960 to 1971 and Joint Ice Center in 1970), visual and radar aircraft observations [Russian (1950–70), American (1960–70), and Norwegian (1963–2005)], ship observations, and observations from land stations [Bjørnøya, Hopen, Isfjord Radio, and Jan Mayen since 1963; see Loyning et al. (2003) for further details]. Up to 10 different ice types have been recorded each week, classified after their mean sea ice concentration. Time series of the different ice types and more details can be found in Kvingedal (2005). The sea ice data are now available in ArcView shapefile format (see online at http://acsys.npolar.no/ahica/gis.htm).

The Barents Sea ice area in this study is bounded by 85°N, 80° and 20°E (Fig. 1). The ocean areas to the west of 20°E are referred to as the Nordic Seas.

Winter seasonal (DJF) means of total sea ice extent were constructed where all grid cells with a sea ice concentration greater than 15% were counted. The winter anomaly time series was constructed by removing the 1967–2005 winter mean from each winter.

b. Reanalysis

Monthly mean atmospheric fields, including near-surface air temperature (SAT) and mean sea level pressure (MSLP), are the National Centers for Environmental Prediction–National Center for Atmospheric Research (NCEP–NCAR) reanalysis data provided by the National Oceanic and Atmospheric Administration–Cooperative Institute for Research in Environmental Sciences (NOAA–CIRES) Climate Diagnostics Center (Kalnay et al. 1996; Kistler et al. 2001) for the period 1967–2002. Winter seasonal means were constructed based on these monthly fields.

c. Cyclone identification

An algorithm for feature tracking developed by Hodges (1994, 1995, 1996, 1999) has been used to construct storm tracks from the NCEP–NCAR reanalysis data provided by the NOAA–CIRES Climate Diagnostics Center (Kalnay et al. 1996; Kistler et al. 2001). The 850-hPa relative vorticity is used instead of the more often used MSLP because it is not an extrapolated field to any large extent and is influenced less by background flow than fields such as MSLP and geopotential height (Anderson et al. 2003). It also focuses more on smaller-scale synoptic activity than these other fields with the advantage that a higher number of storm trajectories can be identified (Hoskins and Hodges 2002). The relative vorticity at 850 hPa has been calculated from the 6-hourly wind components for the whole Northern Hemisphere for DJF in the period 1948–2002. The retained fields are searched for local extremes, which are the centers for positive vorticity anomalies (cyclones), and the feature points for two consecutive time steps are linked together. A cost function based on track smoothness in terms of changes in direction and speed (Hodges 1995, 1996) is calculated for each possible ensemble of trajectories to find the most likely cyclone tracks. The calculation of the statistical diagnostic fields is performed for the DJF season by the use of spherical nonparametric estimators from the ensembles of wintertime feature tracks (Hodges 1996) and is gridded on an equal-area grid. A more detailed description of the dataset can be found in Sorteberg et al. (2005b, and the references therein).

d. Correlation and degrees of freedom

To reduce spurious correlation due to long-term trends or long-term variability that causes serial correlation in the datasets, the significance levels of the computed correlations are estimated by using the effective number of observations (n_{eff}) formulation of Quenouille (1952) instead of the sample size

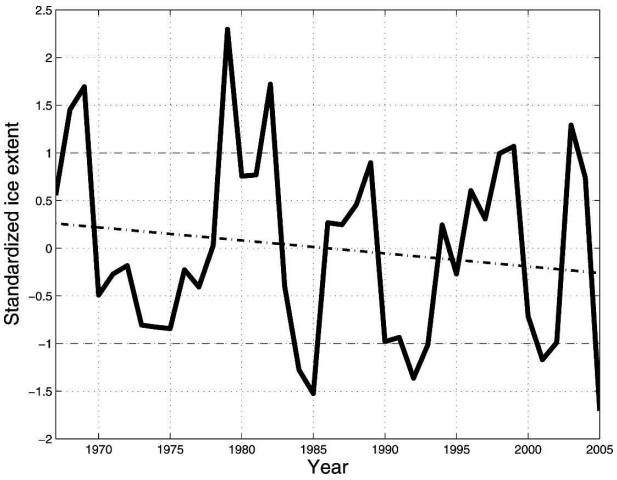

FIG. 2. Standardized Barents Sea winter ice extent during the 1967–2005 period (solid line), ±1 std dev (dashed lines), and the linear trend (dashed–dotted line). The time series is standardized by the removal of its mean value, thereafter divided by its std dev.

$$n_{\text{eff}} = \frac{n}{[1 + 2(r_1 r_1' + r_2 r_2' + \ldots + r_n r_n')]}, \qquad (1)$$

where n is the sample size, and r_1 and r_1' are the lag-1 autocorrelations of the two time series, respectively, r_2 and r_2' are the corresponding lag-2 autocorrelations of the two time series, etc.

For the datasets used in this paper, this typically reduces the degrees of freedom by 15% for the raw data and by 70% for the low-pass-filtered data.

3. The wintertime Barents Sea ice extent

The time series of Barents Sea ice extent during winter shows that there are four distinct periods with above normal sea ice extent (Fig. 2) and a trend in ice extent of −3.5% decade^{-1}. Sharp decreases in the extent between successive winters, such as 1969–70, 1982–83, 1989–90, and 1999–2000, are followed by winters with less-than-normal sea ice extent. Sharp increases, as between 1978–79, 1985–86, and 1993–94, are followed by winters with greater-than-normal sea ice extent. Clearly, there are variations on both interannual and decadal time scales, and spectrum analysis indicates fairly strong variability around the 8- and 3–4-yr periods. The largest deviations from the mean appear in the first half of the 1967–2005 period, manifested in the 1979 winter maximum and the sparse 1985 winter. Despite recent decreases in Barents Sea ice extent, examples of strong variability persist. For example, while 2005 shows the lowest Barents Sea ice extent in our record, the fifth largest Barents Sea ice extent occurred just 2 yr earlier (in 2003).

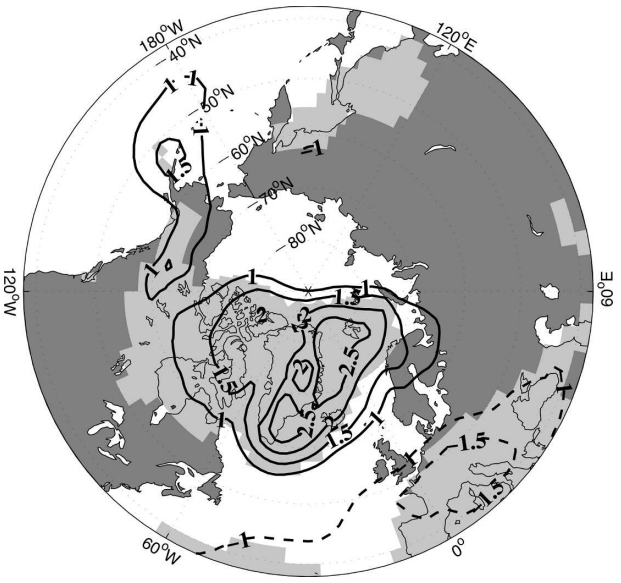

FIG. 3. Linear regression (lines) and areas with significant ($p < 0.1$) correlations (shaded) between wintertime Barents Sea ice extent and wintertime (DJF) MSLP anomalies. Unit of regression: hPa (std dev)$^{-1}$. Calculations performed on the 1967–2002 period.

4. The relationship between Barents Sea winter ice extent and MSLP

Regression analysis (Fig. 3) indicates that during winters with extensive Barents Sea ice, the MSLP is generally higher than during winters with sparse sea ice extent both in the Nordic Seas and in the Barents Sea region. However, the structure is similar with a low pressure center south of Greenland (the Icelandic low) and a low pressure tongue stretching over the Nordic Seas and into the western part of the Barents region, where a secondary pressure minimum is centered. In addition to the MSLP being higher during extensive sea ice years, the east–west pressure gradient in the Nordic Seas is considerably weakened with the strongest increase in MSLP in the western part of the Nordic Sea (between Iceland and the eastern coast of Greenland). In addition, the low pressure center south of Greenland is shifted slightly southwestward. Maximum correlations ($r > 0.4$) between the DJF Barents Sea ice extent and DJF MSLP are seen over eastern Greenland, the Ellesemere and Baffin Islands, central southern Europe, and more surprisingly, south of the Sea of Okhotsk (Fig. 3). This will be investigated in more detail in section 6.

The MSLP anomalies during winters with extensive Barents Sea ice extent reveal higher-than-normal MSLP over Greenland, hence a weakening of the westerlies. More locally in the Barents region, this leads to

TABLE 1. Correlations between DJF Barents Sea ice extent and DJF NAO/AO for the period 1967–2002. The decadal data are low-pass-filtered sea ice extent vs the low-pass-filtered NAO and AO indexes. The filtering is done by using a third-order Butterworth low-pass filter that retains the variability on scales longer than 7 yr. Bold characters indicate that the correlation has a $p < 0.05$ and italic indicate a $p < 0.1$ using a Student's t test with serial correlation taken into account [Eq. (1)].

	Linear correlation	
	Raw data	Decadal variability
NAO	*−0.36*	**−0.63**
AO	*−0.29*	*−0.51*

southward anomalous geostrophic winds. This cold northerly wind favors freezing due to both thermodynamic freezing at the sea ice edge and the breakup and divergence of ice leading to open-water sea ice formation. In addition, these northerly winds may advect more and thicker sea ice into the Barents region from just north of Greenland. The ice north of Greenland is the thickest in the Arctic and even if this ice melts before its arrival in the Barents Sea, it will deposit a large volume of surface freshwater in the Barents Sea, enhancing the likelihood of new ice formation in the region. During sparse sea ice winters, the picture is reversed, and a stronger east–west gradient in the MSLP anomalies (Fig. 3) favors southerly geostrophic wind anomalies over the southern Nordic Seas. This may contribute to the increased inflow of warm, saline Atlantic water into the Nordic Seas. Over the Barents Sea, advection of warm and humid air, which disfavors freezing, will contribute to a reduced sea ice extent by dynamically pushing the sea ice northward and keeping the thick ice (and therefore freshwater) confined to the area north of Greenland.

The MSLP anomaly pattern resembles some of the NAO pattern (Hurrell 1995). The NAO accounts for more than one-third of the total variance in winter SLP in the North Atlantic and has had a pronounced place in the sea ice literature over the last decade. Its impact on the Arctic Ocean is thoroughly discussed in Dickson et al. (2000), and Rigor et al. (2002) discuss the response and motion of sea ice in the Arctic to variability in the AO. Table 1 summarizes the correlations with the NAO index [mean difference of normalized SLP between Ponta Delgada, Azores, and Stykkisholmur, Iceland (Hurrell 1995)] and the more hemispheric-wide AO index (Thompson and Wallace 1998). Neither the time series of the raw NAO index nor the AO index correlate strongly with the winter Barents Sea ice extent (−0.36 and −0.29, respectively). As the NAO/AO can be used as a measure of the strength of the North

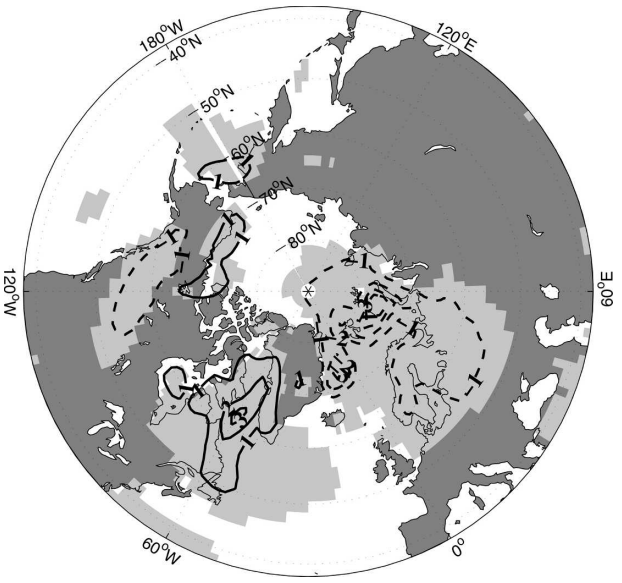

FIG. 4. Same as in Fig. 3, but for wintertime (DJF) 2-m temperature anomalies. Unit of regression: °C (std dev)$^{-1}$.

Atlantic westerlies, this indicates that the direct influence of the North Atlantic westerlies on the Barents Sea ice is fairly weak. An explanation of the relatively weak correlations may be that the NAO/AO index is less well suited for capturing important meridional wind anomalies that may be important for the wintertime Barents Sea ice extent. By applying a third-order Butterworth filter to the time series of Barents Sea winter ice extent, AO, and NAO, the decadal (7-yr low-pass filter) variations were separated. This shows that the decadal variability in the NAO correlates significantly (−0.60) with the decadal Barents Sea winter ice extent.

Vinje (2001a) and Kwok (2000) found a stronger correlation between the April sea ice extent and the winter NAO index, indicating a lagged relation. More so, Vinje (2001a) pointed out that the correspondence between the April Barents Sea ice extent and the NAO winter index during 1864–1996 had different strengths during different subperiods. The periods 1900–35 and 1966–96 excelled with the highest correlations (0.56 and 0.63, respectively). In both these periods, the NAO values were high and persistent for some years, in contrast to the other two periods with smaller and more rapid variations.

5. The relationship between Barents Sea winter ice extent and temperature

The regression of DJF Barents Sea ice extent on DJF 2-m temperature (SAT) anomalies (Fig. 4) shows large

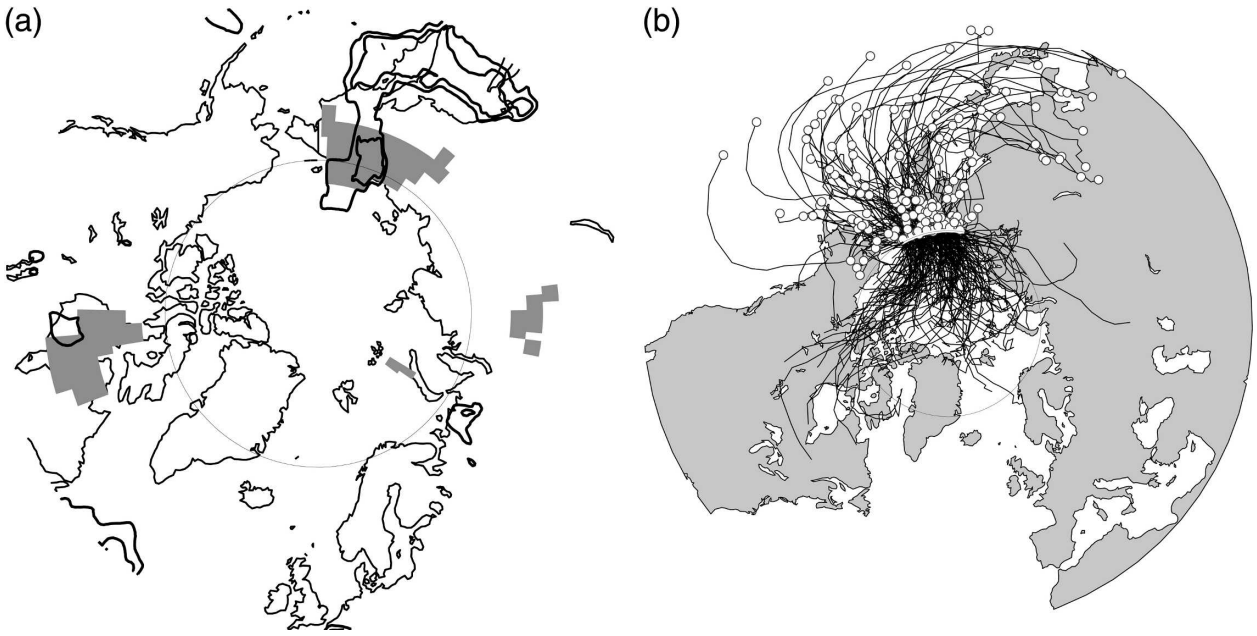

FIG. 5. (a) Areas with significant correlation between the DJF track density (lines)/track genesis (shaded) and the DJF Barents Sea ice extent. Outer and inner lines indicate the 90% and 95% significance levels, respectively. Shading indicates the 90% significance level. (b) The trajectories (lines) and starting points (circles) of northward-moving winter cyclones crossing 70°N between 140°E and 180°. Calculations performed on the 1967–2002 period.

positive (negative) values in the Barents and Nordic Seas during winters with sparse (extended) sea ice. In the Barents Sea, the SAT anomalies exceed 3°C during winters with ice extent anomalies of −1 standard deviation (std dev). This implies that the sea ice edge strongly influences the local SAT (correlation of −0.75). In winters with relatively little Barents Sea ice, the SAT is constrained to the underlying ocean temperatures. During heavy ice winters, the SATs are effectively insulated from the effect of the warmer ocean and are more free to fluctuate in response to other influences. In the Labrador Sea, the signs of the anomalies are reversed (correlation of 0.5–0.65). Outside these regions, SAT anomalies exceeding 1°C followed by significant correlations (Fig. 4) are detected over the Beaufort Sea, the Rocky Mountains, and in the Bering Sea, indicating that the Barents Sea ice extent variability covary with circulation changes that are not only local. As a consequence of the lack of cross–Bering Strait MSLP anomaly gradients during sparse sea ice winters, the SAT anomalies over the Rocky Mountains and Bering Sea are much weaker than the anomalies during extensive Barents Sea ice extent. In this paper, no information is given on the sea ice in the Labrador and Bering Seas. However, the MSLP and SAT anomalies related to the Barents Sea ice extent indicate a connection between the ice extent in the Barents Sea area and the Labrador and Bering Sea ice extent. The dipole pattern in sea ice concentration anomalies between the Labrador Sea and the Nordic and Barents Seas is well known (Walsh and Johnson 1979; Slonosky et al. 1997).

6. The relationship between Barents Sea winter ice extent and cyclone variability

The MSLP regression and correlation pinpoint the general MSLP structure that influences and covaries with the Barents Sea ice extent. However, this gives only limited information on the actual atmospheric processes and time scales that are involved in the variability. To shed some light on the role of cyclone formation and cyclone track variability in the variability of the Barents Sea ice extent, we have used a feature tracking method (see the section "Data and methods") to calculate the wintertime (DJF) track genesis (where the cyclone forms) and track density (number of cyclones) and have correlated the gridded Northern Hemisphere track genesis and track density with the Barents Sea ice extent data. In addition, a lead–lag correlation analysis was performed.

a. East Siberian cyclones

The DJF linear correlation analysis (Fig. 5a) indicates areas where the track density and track genesis

significantly correlate with the wintertime Barents Sea ice extent. For track density, the only area where the correlation exceeds the 95% significance level is over the Sea of Okhotsk and in northern East Siberia. In addition, the track genesis in East Siberia (shaded area in Fig. 5a) significantly correlates with the Barents Sea ice extent. Both the increased (reduced) local formation and higher (lower) number of cyclones in this region during years of higher (lower)-than-normal sea ice extent in the Barents Sea draw our attention to this area.

In order for a cyclone generated or traveling through the East Siberian (ES) region to have an effect on the Barents Sea ice extent, it should be moving into the Arctic region. Thus, we select the northward-moving cyclones crossing 70°N between 140°E and 180° to further study the possible effect of East Siberian cyclone activity on the Barents Sea ice extent. The trajectories of all winter cyclones satisfying this criteria are displayed in Fig. 5b. Seemingly, the cyclones do not have any preferred pathways—cyclones in the easternmost part of the transect (close to 180°) have a tendency to go into the Beaufort Sea while cyclones in the western part of the transect tend to travel into the central Arctic–Kara and Laptev Sea. Only a few of the cyclones actually reach the Barents Sea ice edge. However, the trajectories indicate the movement of the cyclone centers, thus, the atmospheric conditions over the Barents Sea may be influenced by the wind field surrounding the low pressure centers. In addition, the wind field induced by the cyclones affects the sea ice motion in the Arctic Ocean, and thereby the amount of ice moving into the Barents Sea region. On average, 5.8 northward-moving cyclones cross the defined East Siberian transect each winter and stay within the Arctic (north of 70°N) for 2.8 days. Assuming that these cyclones are only affecting the Arctic Ocean when their center is inside the Arctic indicates that on average, around 20% of the winter days may be influenced by a cyclone reaching the Arctic through the East Siberian region. During a winter with maximum East Siberian cyclone activity (15 individual cyclones), this increases to 50% of the days.

During years of extensive ice extent, the larger-than-average number of cyclones that are generated north of the mountain areas in East Siberia and the larger number of cyclones that travel over East Siberia and into central parts of the Arctic create significant southerly wind anomalies in the Bering Strait (Fig. 6). The increased number of East Siberian cyclones also directly contributes or generates favorable conditions for strong northerly wind anomalies in the Kara and Barents Sea region (Fig. 6). The significantly stronger northerly winds over the Barents Sea are favorable for local freezing due to both thermodynamic freezing at the sea ice edge and the breakup and divergence of ice leading to open-water sea ice formation. In addition, the westerly wind anomalies north of the Barents Sea will increase the advection of thick ice into the region due to increased Ekman transport.

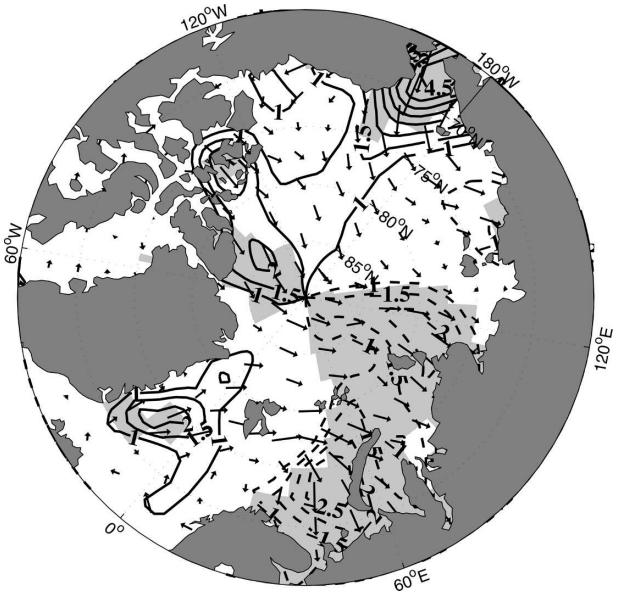

FIG. 6. Composites showing the difference in wind direction (arrows) and change in the meridional wind component (contours) between years with high (>1 std dev) and low (<−1 std dev) numbers of northward-moving winter cyclones crossing 70°N between 140°E and 180°. Shading indicates significant ($p < 0.1$) changes in the meridional wind component.

There is large interannual variability in the number of cyclones that enter the Arctic Ocean from East Siberia, with maxima in 1979 and 1982 counting 15 winter cyclones and a minimum in 1995 with no cyclones. The three winters with the most cyclone activity in the East Siberian region coincide with the three most extensive Barents Sea ice winters (see Fig. 2). In 1995 when no cyclones were observed, the ice extent in the Barents Sea was normal, whereas the minimum Barents Sea ice extent in 1985 coincided with a minima in ES cyclones. The high and positive correlation coefficient (0.63; Table 2) between the northward-traveling cyclones and the Barents Sea ice extent quantifies the relationship. The covariability is particularly pronounced during winters with a larger-than-average number of cyclones. The trend line in Fig. 7 reveals a decrease in the number of northward-moving cyclones in the East Siberian transect during the 1967–2002 period. One might speculate if this has contributed to the decrease in the observed Barents Sea ice extent.

TABLE 2. Correlations between DJF Barents Sea ice extent and DJF cyclone indices for the period 1967–2002. Decadal filtering and significance indicated as in Table 1. NOR represents western Nordic Sea cyclones moving northward and crossing 60°N between 55° and 15°W. ES represents East Siberian cyclones moving northward and crossing 70°N between 140°E and 180°.

	Linear correlation			
Area	Raw data	Raw data and ice lag by 2 yr	Decadal variability	Decadal variability and ice lag by 2 yr
NOR	*−0.29*	**−0.38**	**−0.63**	**−0.89**
ES	**0.63**	0.14	**0.64**	0.17

b. Western Nordic Sea cyclones

Surprisingly, the Nordic Sea cyclone density was found to be only weakly correlated to the Barents Sea ice extent. However, the lead–lag correlation analysis between the Barents Sea ice extent and track genesis/track density revealed significant correlations in the western NOR when the Barents Sea ice extent lags the western Nordic Seas cyclone activity by 1–2 yr (Fig. 8a).

For cyclones in the western Nordic Seas area, we only investigate the fate of the northward-moving cyclones crossing 60°N between 55° and 15°W. Figure 8b displays the trajectories of all winter cyclones satisfying this criteria. Most of these cyclones end up in the Nordic Seas, Scandinavia, or the Barents Sea.

The number of northward-moving winter cyclones in the western Nordic Seas is highly variable, ranging from only 5 in 1977 to 33 (the highest) in 1992 (Fig. 9). As Table 2 shows, the correlation between these winter cyclones and Barents Sea ice extent is negative (−0.29) and only marginally significant. However, as indicated in Fig. 8, when the Barents Sea ice extent time series lags the western Nordic Seas cyclone count time series, the correlation increases to −0.38. The larger negative lag correlation indicates that high (low) activity in northward-moving cyclones in the western Nordic Seas area may be followed by sparse (extensive) Barents Sea winter ice extent 1–2 yr later.

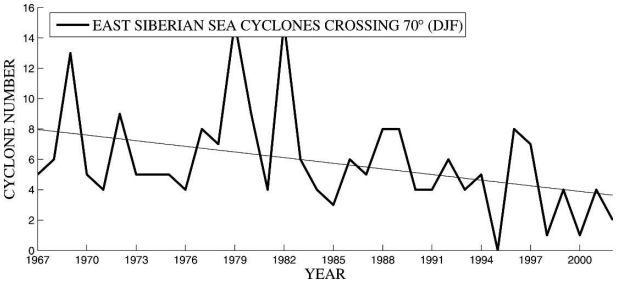

FIG. 7. Number of northward-moving DJF cyclones crossing 70°N between 140°E and 180° and the trend line for the 1967–2002 period.

As seen in Fig. 10, a reduced number of cyclones in the western Nordic Seas will contribute to northeasterly wind anomalies in the Nordic Seas, but there is no significant change in the wind field over the Barents Sea area. The strong correlation when the ice lags 2 yr indicates that the cyclones in these areas are mainly influencing the Barents Sea winter ice extent through its impact on the variability of the inflow of warm, saline Atlantic water to the Barents Sea.

c. Combined cyclone and sea ice variability

As an approach to quantify the sum of the total direct or indirect impact of the wintertime variability in northward-moving cyclones crossing East Siberia and the western Nordic Seas on the Barents Sea ice extent, we try to estimate the Barents Sea ice variability using linear multiple regression, where the cyclone number variabilities in the two previously defined transects (cyclones crossing 70°N between 140°E and 180° and cyclones crossing 60°N between 55° and 15°W) are taken as the predictors. As the correlation analysis indicates, there is a 1–2-yr lag between the western Nordic Seas cyclone variability and the Barents Sea ice response. Therefore, in the multiple regression analysis, we give the western Nordic Seas cyclone time series a 2-yr lead. A large amount of the Barents Sea ice extent variability covaries (correlation is 0.68) with the cyclone activity in the two areas (Fig. 11).

To gain some insight into the covariability between the decadal fluctuations in the Barents Sea ice extent and the cyclone activity, the decadal component (7 yr low-pass filtered) of the Barents Sea winter ice extent variability was constructed using a third-order Butterworth filter and compared to the decadal component of the cyclone activity.

In contrast to the total variability, the decadal variability in the wintertime Barents Sea ice extent seems related to both the East Siberian and western Nordic Sea cyclone variability (Table 2). The relationship is particularly pronounced when the decadal Barents Sea winter ice variability lags the cyclone number variability in the latter area by 2 yr (correlation of −0.89).

Using the decadal cyclone number variability over the western Nordic Sea area with a 2-yr lag (2 yr prior to the ice variability) together with the decadal cyclone number variability over the East Siberian region as predictors, 79% of the decadal cyclone variability covaries with the decadal Barents Sea ice extent variability (Fig. 12). This is not higher than the covariability using only the 2-yr lagged western Nordic Sea cyclones (Table 2), but a separation between the influence of the 2-yr-

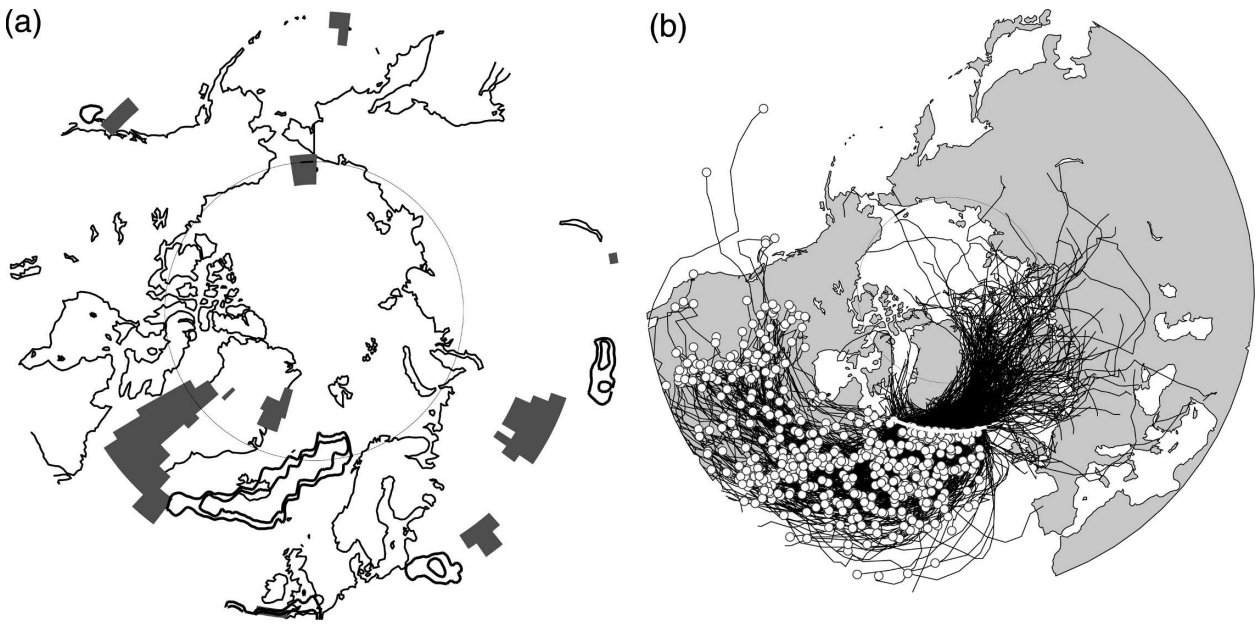

FIG. 8. (a) Areas with significant 2-yr lag correlation between the DJF track density (lines)/track genesis (shaded) and the lagged DJF Barents Sea ice extent. Outer and inner lines indicate the 90% and 95% significance levels, respectively. Shading indicates the 90% significance level. (b) The trajectories (lines) and starting points (circles) of northward-moving winter cyclones crossing 60°N between 55° and 15°W. Calculations performed on the 1967–2002 period.

lagged Nordic Sea and East Siberian cyclones is made difficult since they are not independent predictors (their decadal variability is significantly correlated). It is a very close fit between the estimated and the observed sea ice variability in the first part of the time series and a slight phase shift in the latter part. Using a lag of 1 instead of 2 yr gives the opposite result, indicating that the response time between the Nordic cyclone variability and the Barents Sea ice extent may range between 1 and 2 yr.

7. Discussion and conclusions

This investigation of the wintertime atmospheric forcing on the Barents Sea winter ice extent aims to contribute to a better understanding of the actual processes acting on the ice on different time scales. The sea ice dataset used has at least two important properties that make it suitable for this study. The long period of data (1967–2005), making decadal variability detectable, and its high temporal resolution. By studying weekly ice maps, strong short-term ice extent fluctuations are captured and accounted for when the average

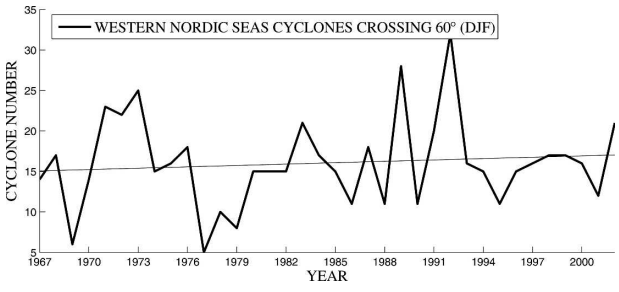

FIG. 9. Same as in Fig. 7, but for 60°N between 55° and 15°W.

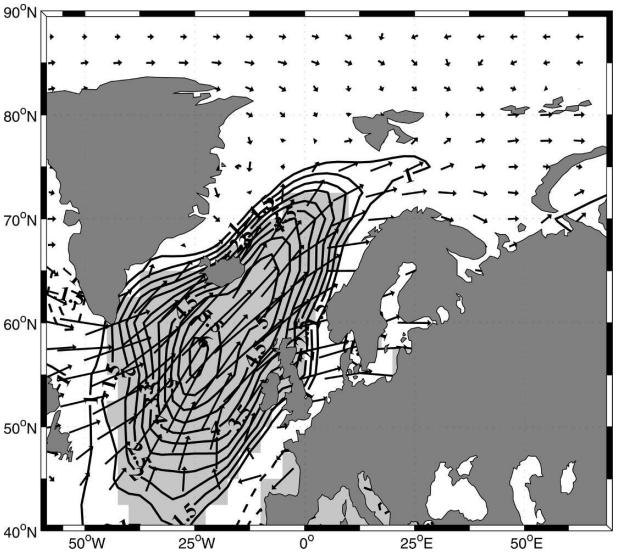

FIG. 10. Same as in Fig. 6, but composites based on northward-moving cyclones crossing 60°N between 55° and 15°W.

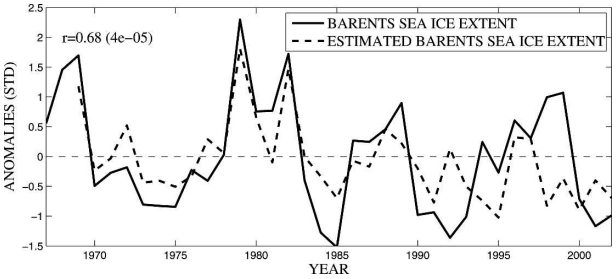

FIG. 11. Observed Barents Sea winter ice extent and the estimated Barents Sea winter ice extent derived using the variability in cyclone activity in the ES area (northward-moving cyclones crossing 70°N between 140°E and 180°) together with the 2-yr leading variability in cyclone activity in the western Nordic Sea area (cyclones crossing 60°N between 55° and 15°W) as predictors. Here, r is the correlation between the observed and estimated values with the p value in parantheses.

wintertime ice extent is calculated. The time series of Barents Sea winter ice extent reveals strong interannual variability and a slightly decreasing trend of −3.5% decade^{-1}, with the winter of 2005 marking a new record low in the wintertime Barents Sea ice extent.

Though the regression and linear correlation analysis do not give any real insight into the causal relationship between the Barents Sea winter ice extent and MSLP or cyclone track variability, we propose the following synoptic mechanism to be important for the interannual Barents Sea winter ice extent variability: The variability in the number of northward-moving cyclones in the East Siberian region results in the variability in the number of cyclones traveling into the central Arctic, and the Siberian, Laptev, and Kara Seas. This influences the winds over the central Arctic, the Laptev, and the Barents Sea region, which in turn influences both the sea ice export and local production of ice in the Barents Sea region. Years with a high production of cyclones over East Siberia favor northwesterly wind anomalies bringing cold air over the Laptev and Barents Sea area. These changes favor ice export into the Barents Sea area. The wind anomalies are also favorable for local freezing due to both thermodynamic freezing at the sea ice edge and the breakup and divergence of ice leading to open-water sea ice formation. It should be noted that there is a notable reduction in the northward-moving cyclones coming from the East Siberian region with time. This may have contributed to the reduction in wintertime sea ice extent seen in the Barents Sea region.

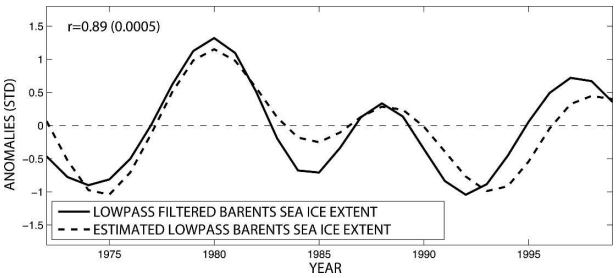

FIG. 12. Same as in Fig. 11, but for observed decadal Barents Sea winter ice extent using the decadal variability. The data were low-pass filtered using a Butterworth filter with a cutoff of 7 yr before a linear multiple regression was calculated.

Whether the cyclones themselves are responsible for the wind anomalies seen in the Barents Sea or if they are just triggering other mechanisms that lead to cold air outbreaks or other phenomena that favor northwesterly flow over the Barents Sea is not clear. It is also not possible to exclude the possibility that the covariability seen between the East Siberian cyclones and the Barents Sea ice extent is related to a common yet unknown forcing, possibly related to the variability in atmospheric planetary waves that might give favorable conditions for both cyclone formation in East Siberia and strong wind anomalies in the Barents Sea. One mechanism that has been proposed to be important for the Arctic circulation in general (Cavalieri and Häkkinen 2001) and the Fram Strait sea ice export in particular (Cavalieri 2002) is the phase of the planetary-scale sea level pressure wave 1. However, we note that 2 of the 3 yr of maximum East Siberian cyclone variability (1969, 1979) coincide with years with small amplitudes (less than 20% of the first 6 zonal wavenumbers) in the zonal planetary wave-1 pattern (Cavalieri and Häkkinen 2001, their Fig. 1a).

A local positive feedback between the Barents Sea ice extent and the local cyclone formation was proposed by Bengtsson et al. (2004). Reduced ice extent was suggested to favor local cyclone production, which might (if the locally produced cyclones stay in the Barents Sea) cause northwesterly wind anomalies in the area of Barents Sea inflow and therefore the increased inflow of Atlantic water. A strong feedback was indeed found with a correlation of −0.81 between the decadal Barents Sea ice extent and the local cyclone genesis (reduced to −0.32 for the unfiltered data). However, for the time period investigated here, this positive feedback seems secondary to the strong forcing given by the variability in cyclones in East Siberia and the Nordic Seas since the cyclones produced locally were moving out of the Barents Sea region (mainly into Russia) quite rapidly.

The decadal variability in the Barents Sea ice extent is strongly governed by the decadal variability in the number of cyclones entering the Nordic Seas, with the ice extent lagging by 1–2 yr.

The decadal variability of the Nordic Seas cyclone activity induces wind anomalies in the North Atlantic and the Nordic Seas. This mechanism is of great importance for the decadal ice extent variations, as it influences the heat transport in the ocean in two ways:

1) The influence on the dynamics of the Nordic Seas ocean circulation through modulating the variability in the inflow of Atlantic water to the Nordic Seas, and in addition the width and location of the Atlantic water
2) Variability in the advection of warm air into the Nordic Seas, which will modulate the heat loss from the ocean and therefore be an important factor in determining the amount of heat transported by the ocean into the Barents Sea area.

The first point is supported by several studies (e.g., Nilsen et al. 2003; J. Zhang et al. 2004) relating the volume and heat flow into the Nordic Seas to the NAO variability. In addition, Sorteberg et al. (2005b) showed a strong influence of the wintertime Nordic Seas cyclonic activity on the wintertime volume net flow of Atlantic water into the Nordic Seas. The relationship between the Atlantic inflow and the Nordic Seas cyclones was most apparent during time periods where there was a significant decadal component in the cyclone variability (after the 1970s), leading to an atmospheric forcing of the same sign over several years. Two mechanisms were proposed that may contribute to this increased covariability during decades with a strong long-term signal (Sorteberg et al. 2005b). The first is the general increase in the Nordic Seas cyclone variability during this period, which could lead to a nonlinear impact (the wind stress is approximately proportional to the square of the wind speed) of the cyclone variability on the oceanic volume transports. This could make the covariability between the variability in the cyclones and the oceanic volume transports more apparent during years with strong cyclone variability. The second effect might be that a stronger persistence in the storm track due to increased variability on decadal scales could impose a forcing of the same sign on the ocean for a longer period and therefore make the faster barotropic and slower baroclinic ocean adjustments work together during periods of strong decadal variability. The reduced covariability between Nordic Sea cyclone activity and the inflow of Atlantic water into the Nordic Seas during years with reduced decadal cyclone variability (correlation was less than 0.4 from the 1950s to the 1970s and increased to over 0.7 from 1970 to the mid-1990s) should act as a warning to extrapolate the findings in this paper to earlier decades where the decadal signal may be less pronounced.

The inflow of heat into the Nordic Seas is closely related to Atlantic water penetration farther into the Arctic at the Fram Strait and through the Barents Sea (Karcher et al. 2003). During years of strong cyclonic activity in the Nordic Seas, the front between the polar waters to the west of the Nordic Seas and the Atlantic water to the east is displaced toward the Norwegian coast (Blindheim et al. 2000), as is the Atlantic water itself (Mork and Blindheim 2000). Due to topographical steering and a narrower current, more warmer Atlantic water will be transported into the Arctic Ocean, and model simulations indicate that the major part of the increased transport will occur through the Barents Sea (Zhang et al. 1998), which may affect the decadal variations in the Barents Sea winter ice extent.

It should, however, be noted that the origin of the heat anomalies traveling into the Barents Sea region is still unclear. Some studies indicate no correlation between observed SST anomalies in the North Atlantic (south of Iceland) and SST anomalies in the Nordic Seas (Hansen and Bezdek 1996; Sutton and Allen 1997), suggesting that the SST anomalies are either generated within the Nordic Seas or advected upward from deeper into the water column. Furevik (2000, 2001) conducted a detailed study of two warm (first seen in 1982 and 1987) and one cold (first seen in 1984) SST anomalies traveling northward along the Norwegian coast. The anomalies were seen in the Scotland–Faroe section (~58°N) 1–2 yr before they reached the Barents Sea entrance (the Bjørnøya–Fugløya section, ~71°N). This corresponds well with the strongest Barents Sea ice extent anomalies in this period happening 1–2 yr after the beginning of these SST events (1983–85, 1986–89, and 1991–93) and supports our finding of a 1–2-yr lag between the cyclone decadal variability and the Barents Sea winter ice extent variability.

Interestingly, the studies conclude that the ocean heat anomalies amplify (relative to their surroundings) along the Norwegian coast. This supports our second point that the atmospheric effect on the ocean is not just the effect of increased southwesterly winds and the increased inflow of water, but also advection of warmer air into the region, which reduces the heat loss from the northward-traveling ocean heat anomalies.

It is uncertain whether the Atlantic Ocean heat anomalies influence the decadal variability of the cyclonic activity or not. Investigating the temporal covariance between monthly North Atlantic SSTs and 500-hPa geopotential height anomalies, Czaja and Frankignoul (2002) found a possible positive feedback from the ocean that might explain up to 15% of the monthly NAO variance. However, this result may be an artifact

of the persistence (winter-to-winter memory) in the NAO caused by other as yet unknown mechanisms.

The NAO index may be seen as an index containing information on the variability in sea level pressure on all spatial scales ranging from the planetary to synoptic, and is therefore linked to the Nordic Seas cyclone variability. In the time period studied here, the fraction of the northward-moving western Nordic Seas cyclone variance that covaries with the NAO DJF index (Hurrell 1995) is 23% (increased to 70% for the decadal component). Thus, any findings related to the NAO inherently include some of the cyclone variability studied here. However, even though the relationship between the wintertime NAO and the Nordic Seas cyclones is fairly strong in the period studied here, it broke down in the 1960s, indicating that the DJF NAO index should be used with some caution as a proxy for the Nordic Seas cyclone variability (Sorteberg et al. 2005b).

Acknowledgments. This work was supported by the Norwegian Research Council's NORKLIMA program through the NESSAS Grant. We thank Dr. K. Hodges at the University of Reading for providing the cyclone tracking algorithm. This is Publication Number A 119 from the Bjerknes Centre for Climate Research.

REFERENCES

Anderson, D., K. I. Hodges, and B. J. Hoskins, 2003: Sensitivity of feature-based analysis methods of storm tracks to the form of background field removal. *Mon. Wea. Rev.,* **131,** 565–573.

Andreas, E. L, 1980: Estimation of heat and mass fluxes over Arctic leads. *Mon. Wea. Rev.,* **108,** 2057–2063.

Bengtsson, L., V. A. Semenov, and O. M. Johannessen, 2004: The early twentieth-century warming in the Arctic—A possible mechanism. *J. Climate,* **17,** 4045–4057.

Blindheim, J., V. Borovkov, B. Hansen, S. A. Malmberg, B. Turrell, and S. Østerhus, 2000: Upper layer cooling and freshening in the Norwegian Sea in relation to atmospheric forcing. *Deep-Sea Res.,* **41,** 655–680.

Cavalieri, D. J., 2002: A link between Fram Strait sea ice export and atmospheric planetary wave phase. *Geophys. Res. Lett.,* **29,** 1614, doi:10.1029/2002GL014684.

——, and S. Häkkinen, 2001: Arctic climate and atmospheric planetary waves. *Geophys. Res. Lett.,* **28,** 791–794.

Comiso, J., P. Wadhams, L. T. Pedersen, and R. A. Gersten, 2001: Seasonal and interannual variability of the Odden ice tongue and a study of environmental effects. *J. Geophys. Res.,* **106,** 9093–9116.

Czaja, A., and C. Frankignoul, 2002: Observed impact of Atlantic SST anomalies on the North Atlantic Oscillation. *J. Climate,* **15,** 606–623.

Deser, C., J. E. Walsh, and M. S. Timlin, 2000: Arctic sea ice variability in the context of recent atmospheric circulation trends. *J. Climate,* **13,** 617–633.

——, M. Holland, G. Reverdin, and M. Timlin, 2002: Decadal variations in Labrador Sea ice cover and North Atlantic sea surface temperatures. *J. Geophys. Res.,* **107,** 3035, doi:10.1029/2000JC000683.

Dickson, R. R., and Coauthors, 2000: The Artic Ocean response to the North Atlantic Oscillation. *J. Climate,* **13,** 2671–2696.

Furevik, T., 2000: On anomalous sea surface temperatures in the Nordic Seas. *J. Climate,* **13,** 1044–1053.

——, 2001: Annual and interannual variability of Atlantic Water temperatures in the Norwegian and Barents Seas: 1980–1996. *Deep-Sea Res.,* **48,** 383–404.

Hansen, D. V., and H. F. Bezdek, 1996: On the nature of decadal anomalies in North Atlantic sea surface temperature. *J. Geophys. Res.,* **101,** 8749–8758.

Hassol, S. J., 2004: *Impacts of a Warming Arctic: Arctic Climate Impact Assessment.* Cambridge University Press, 139 pp.

Hodges, K. I., 1994: A general method for tracking analysis and its application to meteorological data. *Mon. Wea. Rev.,* **122,** 2573–2586.

——, 1995: Feature tracking on the unit sphere. *Mon. Wea. Rev.,* **123,** 3458–3465.

——, 1996: Spherical nonparametric estimators applied to the UGAMP model integration for AMIP. *Mon. Wea. Rev.,* **124,** 2914–2932.

——, 1999: Adaptive constraints for feature tracking. *Mon. Wea. Rev.,* **127,** 1362–1373.

Hoskins, B. J., and K. I. Hodges, 2002: New perspectives on the Northern Hemisphere winter storm tracks. *J. Atmos. Sci.,* **59,** 1041–1061.

Houghton, J. T., Y. Ding, D. J. Griggs, M. Noguer, P. J. van der Linden, X. Dai, K. Maskell, and C. A. Johnson, Eds., 2001: *Climate Change 2001: The Scientific Basis.* Cambridge University Press, 881 pp.

Hurrell, J. W., 1995: Decadal trends in the North Atlantic Oscillation: Regional temperatures and precipitation. *Science,* **269,** 676–679.

Johannessen, O. M., E. V. Shalina, and M. W. Miles, 1999: Satellite evidence for an Arctic sea ice cover in transformation. *Science,* **286,** 1937–1939.

Kalnay, E., and Coauthors, 1996: The NCEP/NCAR 40-Year Reanalysis Project. *Bull. Amer. Meteor. Soc.,* **77,** 437–471.

Karcher, M., R. Gerdes, F. Kauker, and C. Koberle, 2003: Arctic warming: Evolution and spreading of the 1990s warm event in the Nordic Seas and Arctic Ocean. *J. Geophys. Res.,* **108,** 3034, doi:10.1029/2001JC001265.

Kistler, R., and Coauthors, 2001: The NCEP–NCAR 50-Year Reanalysis: Monthly means CD-ROM and documentation. *Bull. Amer. Meteor. Soc.,* **82,** 247–267.

Krahmann, G., and M. Visbeck, 2003: Variability of the northern annular mode's signature in winter sea ice concentration. *Polar Res.,* **22,** 51–57.

Kvingedal, B., 2005: Sea ice extent and variability in the Nordic Seas, 1967–2002. *The Nordic Seas: An Integrated Perspective, Geophys. Monogr.,* Vol. 158, Amer. Geophys. Union, 137–156.

Kwok, R., 2000: Recent changes in Arctic Ocean sea ice motion associated with the North Atlantic Oscillation. *Geophys. Res. Lett.,* **27,** 775–778.

——, G. F. Cunningham, and S. S. Pang, 2004: Fram Strait sea ice outflow. *J. Geophys. Res.,* **109,** C01009, doi:10.1029/2003JC001785.

Liu, J., J. A. Curry, and Y. Hu, 2004: Recent Arctic sea ice variability: Connections to the Arctic Oscillation and the ENSO. *Geophys. Res. Lett.,* **31,** L09211, doi:10.1029/2004GL019858.

Loyning, T., C. Dick, H. Goodwin, O. Pavlova, T. Vinje, G.

Kjærnli, and T. Villinger, 2003: ACSYS historical ice chart archive (1553–2002). IACPO Informal Rep. 8, Tromsø, Norway, 32 pp.

Maykut, G. A., 1978: Energy exchange over young sea ice in the central Arctic. *J. Geophys. Res.,* **83,** 3646–3658.

McCabe, G. J., M. P. Clark, and M. C. Serreze, 2001: Trends in Northern Hemisphere surface cyclone frequency and intensity. *J. Climate,* **14,** 2763–2768.

Mork, K. A., and J. Blindheim, 2000: Variation in the Atlantic inflow to the Nordic Seas, 1955–1996. *Deep-Sea Res.,* **47,** doi:10.1016/S0967-0637(99)00091-6.

Mysak, L. A., and S. A. Venegas, 1998: Decadal climate oscillations in the Arctic: A new feedback loop for atmosphere–ice–ocean interactions. *Geophys. Res. Lett.,* **25,** 3607–3610.

——, D. K. Manak, and R. F. Marsden, 1990: Sea-ice anomalies in the Greenland and Labrador Seas during 1901–1984 and their relation to an interdecadal Arctic climate cycle. *Climate Dyn.,* **5,** 111–133.

Nilsen, J. E. Ø., Y. Gao, H. Drange, T. Furevik, and M. Bentsen, 2003: Simulated North Atlantic–Nordic Seas water mass exchanges in an isopycnic coordinate OGCM. *Geophys. Res. Lett.,* **30,** 1536, doi:10.1029/2002GL016597.

Parkinson, C. L., D. J. Cavalieri, P. Gloersen, H. J. Zwally, and J. Comiso, 1999: Arctic sea ice extents, areas, and trends, 1978–1996. *J. Geophys. Res.,* **104,** 20 837–20 856.

Polyakov, I. V., and Coauthors, 2002: Observationally based assessment of polar amplification of global warming. *Geophys. Res. Lett.,* **29,** 1878, doi:10.1029/2001GL011111.

Quenouille, M. H., 1952: *Associated Measurements.* Butterworths Scientific, 242 pp.

Rigor, I. G., J. M. Wallace, and R. L. Colony, 2002: Response of sea ice to the Arctic Oscillation. *J. Climate,* **15,** 2648–2663.

Shuchman, R. A., E. G. Josberger, C. A. Russel, K. W. Fischer, O. M. Johannessen, J. Johannessen, and P. Gloersen, 1998: Greenland Sea Odden sea ice feature: Intra-annual and interannual variability. *J. Geophys. Res.,* **103,** 12 709–12 724.

Simonsen, K., and P. M. Haugan, 1996: Heat budgets of the Arctic Mediterranean and sea surface heat flux parameterizations for the Nordic Seas. *J. Geophys. Res.,* **101,** 6553–6576.

Slonosky, V. C., L. A. Mysak, and J. Derome, 1997: Linking Arctic sea ice and atmospheric circulation anomalies on interannual and decadal time scales. *Atmos.–Ocean,* **35,** 336–366.

Sorteberg, A., T. Furevik, H. Drange, and N. G. Kvamstø, 2005a: Effects of simulated natural variability on Arctic temperature projections. *Geophys. Res. Lett.,* **32,** L18708, doi:10.1029/2005GL023404.

——, N. G. Kvamstø, and Ø. Byrkjedal, 2005b: Wintertime Nordic Seas cyclone variability and its impact on oceanic volume transports into the Nordic Seas. *The Nordic Seas: An Integrated Perspective, Geophys. Monogr.,* Vol. 158, Amer. Geophys. Union, 137–156.

Sutton, R. T., and M. R. Allen, 1997: Decadal predictability of North Atlantic sea surface temperature and climate. *Nature,* **388,** 563–567.

Thompson, D. W. J., and J. M. Wallace, 1998: The Arctic Oscillation signature in the wintertime geopotential height and temperature fields. *Geophys. Res. Lett.,* **25,** 1297–1300.

Vinje, T., 1976: Sea ice conditions in the European sector of the marginal seas of the Arctic, 1966–1975. *Norsk Polarinstitutt Årbok 1975,* Norwegian Polar Institute, 163–174.

——, 1998: On the variation during the past 400 years of the Barents Sea ice edge position and Northern Hemisphere temperatures. *Proc. Symp. on Polar Processes and Global Climate,* Orcas Island, WA, WCRP, 271–273.

——, 2001a: Anomalies and trends of sea-ice extent and atmospheric circulation in the Nordic Seas during the period 1864–1998. *J. Climate,* **14,** 255–267.

——, 2001b: Fram Strait ice fluxes and atmospheric circulation: 1950–2000. *J. Climate,* **14,** 3503–3517.

Walsh, J. E., and C. M. Johnson, 1979: An analysis of Arctic sea ice fluctuations, 1953–1977. *J. Phys. Oceanogr.,* **9,** 580–591.

——, and W. L. Chapman, 1990: Arctic contribution to upper-ocean variability in the North Atlantic. *J. Climate,* **3,** 1462–1473.

Yi, D., L. A. Mysak, and S. A. Venegas, 1999: Decadal-to-interdecadal fluctuations of Arctic sea-ice cover and the atmospheric circulation during 1954–1994. *Atmos.–Ocean,* **37,** 389–415.

Zhang, J., D. A. Rothrock, and M. Steele, 1998: Warming of the Arctic Ocean by a strengthened Atlantic inflow: Model results. *Geophys. Res. Lett.,* **25,** 1745–1748.

——, ——, and ——, 2000: Recent changes in Arctic sea ice: The interplay between ice dynamics and thermodynamics. *J. Climate,* **13,** 3099–3114.

——, M. Steele, D. A. Rothrock, and R. W. Lindsay, 2004: Increasing exchanges at Greenland-Scotland ridge and their links with the North Atlantic Oscillation and Arctic sea ice. *Geophys. Res. Lett.,* **31,** L09307, doi:10.1029/2003GL019304.

Zhang, X., J. E. Walsh, J. Zhang, U. S. Bhatt, and M. Ikeda, 2004: Climatology and interannual variability of Arctic cyclone activity: 1948–2002. *J. Climate,* **17,** 2300–2317.

Zhang, Y., and E. C. Hunke, 2001: Recent Arctic change simulated with a coupled ice-ocean model. *J. Geophys. Res.,* **106,** 4369–4390.